Nephrol Dial Transplant (2014) 29: 313–324
doi: 10.1093/ndt/gft431
Advance Access publication 28 October 2013

KCa3.1 mediates activation of fibroblasts in diabetic renal interstitial fibrosis

Chunling Huang[1,2], Sylvie Shen[1], Qing Ma[1], Anthony Gill[3], Carol A. Pollock[1] and Xin-Ming Chen[1]

[1]Kolling Institute of Medical Research, Sydney medical school and University of Sydney, Royal North Shore Hospital, St Leonards, Sydney, NSW, Australia, [2]Xiamen Center of Clinical Laboratory, Xiamen Zhongshan Hospital, Medical College of Xiamen University, Xiamen, China and [3]Department of Anatomical Pathology, Royal North Shore Hospital, St Leonards, Sydney, NSW, Australia

Correspondence and offprint requests to: Carol A. Pollock; E-mail: carol.pollock@sydney.edu.au

ABSTRACT

Background. Fibroblast activation plays a critical role in diabetic nephropathy (DN). The Ca^{2+}-activated K^+ channel KCa3.1 mediates cellular proliferation of many cell types including fibroblasts. KCa3.1 has been reported to be a potential molecular target for pharmacological intervention in a diverse array of clinical conditions. However, the role of KCa3.1 in the activation of myofibroblasts in DN is unknown. These studies assessed the effect of KCa3.1 blockade on renal injury in experimental diabetes.

Methods. As TGF-β1 plays a central role in the activation of fibroblasts to myofibroblasts in renal interstitial fibrosis, human primary renal interstitial fibroblasts were incubated with TGF-β1 +/− the selective inhibitor of KCa3.1, TRAM34, for 48 h. Two streptozotocin-induced diabetic mouse models were used in this study: wild-type KCa3.1+/+ and KCa3.1−/− mice, and secondly eNOS−/− mice treated with or without a selective inhibitor of KCa3.1 (TRAM34). Then, markers of fibroblast activation and fibrosis were determined.

Results. Blockade of KCa3.1 inhibited the upregulation of type I collagen, fibronectin, α-smooth muscle actin, vimentin and fibroblast-specific protein-1 in renal fibroblasts exposed to TGF-β1 and in kidneys from diabetic mice. TRAM34 reduced TGF-β1-induced phosphorylation of Smad2/3 and ERK1/2 but not P38 and JNK MAPK in interstitial fibroblasts.

Conclusions. These results suggest that blockade of KCa3.1 attenuates diabetic renal interstitial fibrogenesis through inhibiting activation of fibroblasts and phosphorylation of Smad2/3 and ERK1/2. Therefore, therapeutic interventions to prevent or ameliorate DN through targeted inhibition of KCa3.1 deserve further consideration.

Keywords: diabetic nephropathy, fibroblast activation, KCa3.1, renal interstitial fibrosis

ORIGINAL ARTICLE

INTRODUCTION

Diabetic nephropathy (DN) is a major complication of diabetes and a leading cause of death among patients with diabetes mellitus. Recent studies suggest that tubulointerstitial fibrosis is the final common pathway of almost all forms of chronic progressive renal disease, including DN [1]. Tubulointerstitial fibrosis involves expansion of interstitial fibroblasts, myofibroblast activation and extracellular matrix (ECM) accumulation, resulting in the loss of normal kidney function and ultimately renal failure [2]. Regardless of the origin of myofibroblasts, there is common agreement that the myofibroblast is the cell most responsible for interstitial expansion and matrix accumulation during the course of renal fibrosis.

Central to the activation of fibroblasts to profibrotic myofibroblasts is transforming growth factor-β1 (TGF-β1), which exerts its effects via the small mothers against decapentaplegic (Smad) or/and mitogen-activated protein kinase (MAPK) pathways [3]. It is considered that TGF-β1 plays a pivotal role in the pathogenesis of DN [4]. TGF-β1 induces the transcription of genes involved in ECM protein accumulation, including type I collagen and fibronectin. In addition, TGF-β1 stimulates the expression of many ECM proteins in renal cells by stimulating the expression of genes regulating fibrotic process, including plasminogen activator inhibitor-1 (PAI-1) and matrix metalloproteinases (MMPs), thus modifying the matrix degradation process [5–7].

Ca^{2+}-activated K^+ channels can communicate directly from Ca^{2+} signal pathways to changes in membrane potential that are critically required for various cellular processes. The intermediate-conductance calcium-activated K^+ channel KCa3.1 (also known as IK1, SK4 or KCNN4) is present in multiple

cells implicated in progressive fibrosis, including vascular smooth muscle and endothelial cells, T lymphocytes, macrophages and fibroblasts. In each of these cells it regulates calcium signaling and hence membrane potential and participates in the control of cellular functions such as cell proliferation and gene expression [8–12]. KCa3.1 has been reported to be a potential molecular target for pharmacological intervention in a diverse array of clinical conditions including vascular restenosis, urinary incontinence, prostate cancer and autoimmune disease [13–15]. Recently, we have demonstrated that KCa3.1 regulated fibrotic responses in proximal tubular cells in DN [16]. However, the role of KCa3.1 in the activation of fibroblasts to myofibroblasts related to DN has not been studied. To gain further insight into KCa3.1's role in activation of myofibroblast and to identify fibrogenesis in DN in which interfering with KCa3.1 function may be beneficial, we investigated the effects of KCa3.1 on fibroblast activation, matrix synthesis and degradation induced by TGF-β1 in human primary renal interstitial fibroblasts and explored the mechanisms whereby KCa3.1 inhibition suppressed functional and pathological consequences of DN in two mouse models of DN.

ORIGINAL ARTICLE

SUBJECTS AND METHODS

Materials

Recombinant human TGF-β1 and the highly selective KCa3.1 blocker TRAM34 (1-[(2-chlorophenyl) diphenylmethyl]-1H-pyrazole) were purchased from R&D Systems (Minneapolis, MN, USA) and Sigma-Aldrich (St. Louis, MO, USA). Anti-PAI-1 was purchased from BD Biosciences (Franklin Lakes, NJ, USA). Anti-type I and type IV collagen was obtained from Abcam (Cambridge, MA, USA). Anti-fibronectin, anti-α-smooth muscle actin (α-SMA) and anti-α-tubulin antibodies were from Sigma (St. Louis, MO, USA). Anti-phospho-Smad2, anti-phospho-Smad3, anti-Smad2/3, anti-phospho-ERK, anti-ERK, anti-phospho-p38, anti-p38 antibody, anti-phospho-JNK and anti-JNK were purchased from Cell Signaling Technology (Danvers, MA, USA).

Human kidney biopsies and primary cell culture

Human primary renal interstitial fibroblasts were isolated from normal human kidney cortex as previously described [17]. This study was approved by the Human Research Ethics Committee of the Royal North Shore Hospital.

Human renal interstitial fibroblasts were cultured in DMEM/Ham's F12 (Gibco BRL, UK) supplemented with 10% FCS and 1% PSG under standard conditions. All experiments were performed on quiescent and confluent interstitial fibroblasts at passage 2. The cells were exposed to TGF-β1 (2 ng/mL) in the presence or absence of TRAM34 (2 μM) [18, 19] for 48 h and then the culture supernatants, total RNA and cell lysates were collected, respectively. In all experiments, cells were serum starved overnight before adding TGF-β1 and TRAM34.

Animal studies

KCa3.1−/− mice and eNOS−/− mice were used in this study. KCa3.1−/− mice were kindly provided by Dr James Melvin (National Institute of Dental and Craniofacial Research, Bethesda, MD, USA). eNOS−/− mice are regarded as an ideal mouse model of DN, endorsed by the Animal Models of Diabetic Complications Consortium [20]. Eight-week-old male KCa3.1+/+ (C57B/6) mice, KCa3.1−/− mice and eNOS −/−mice (Jackson laboratory, ME, USA) weighing ∼20–25 g were assigned to receive either 55 mg/kg of streptozotocin (STZ) (Sigma, MO, USA) diluted in 0.1 M citrate buffer, pH 4.5, or citrate buffer alone by intraperitoneal injection as described previously [21]. A group of KCa3.1+/+ ($n = 8$) and eNOS−/−mice ($n = 6$) received citrate buffer alone served as non-diabetic controls. eNOS−/− diabetic mice were then randomized into two groups, receiving treatment with TRAM34, 120 mg/kg/day intraperitoneally or vehicle (DMSO) alone for 24 weeks. Treatment commenced within 24 h of the last STZ injection. All animals were housed in the Kearns Animal Facility of Kolling Institute of Medical Research with a stable environment maintained at 22 ± 1°C with a 12/12-h light–dark cycle.

Mice were weighed and their blood glucose levels were measured using Accu-chek glucometer (Roche Diagnostics) weekly and only diabetic animals with blood glucose >16 mmol/L were considered diabetic. Diabetic mice received insulin (Lantus, Germany) treatment to prevent ketosis. At the time of sacrifice, 24-h urines were collected in metabolic cages. Urine albumin levels were determined using the Murine Microalbuminuria ELISA kit (Exocell, Inc., Philadelphia, PA, USA). After animals were culled, the left kidneys were removed and snap frozen for the isolation of RNA or protein, and the right kidneys were perfused with PBS and fixed in 10% buffered formalin for histological examination. Experimental procedures adhered to the guidelines of the National Health and Medical Research Council of Australia's Code for the Care and Use of Animals for Scientific Purposes and were approved by the Animal Research Ethics Committee of Royal North Shore Hospital.

RNA isolation and RT–PCR analysis

Total RNA was extracted from cells and mouse kidneys using GenElute Mammalian Total RNA Miniprep Kit (Sigma) or Trizol (Invitrogen, CA, USA), respectively. The cDNA was synthesized using SuperScript VILO cDNA Synthesis Kit (Invitrogen). Quantitative real-time PCR was performed using the SYBR Green PCR master mix kit (Invitrogen) with the intron-spanning primers as shown in Table 1 on ABI-Prism-7900 Sequence Detection System (Applied Biosystems). The relative mRNA expression levels were calculated according to the $2^{-\Delta\Delta Ct}$ method [22]. The mRNA expression of β-actin was used as the endogenous reference control.

Western blot analysis

Type IV collagen and fibronectin were measured in cell culture supernatant and cell lysates prepared in RIPA buffer with protease inhibitors (Roche, Germany).

Table 1. Nucleotide sequences of the primers used for qRT–PCR

Species	Molecules	Forward primer (5′–3′)	Reverse primer (5′–3′)
Human	α-SMA	CCGACCGAATGCAGAAGGA	ACAGAGTATTTGCGCTCCG
	COL1A	TCTGGAGAGGCTGGTACTGC	GAGCACCAAGAAGACCCTGA
	COL4A1	CGGGTACCCAGGACTCATAG	GGACCTGCTTCACCCTTTTC
	FN	GCGAGAGTGCCCCTACTACA	GTTGGTGAATCGCAGGTCA
	FSP-1	CTTGCACACGCTGTTGCTAT	CGAGTACTTGTGGAAGGTGGA
	GAPDH	AGCCACATCGCTCAGACAC	GCCCAATACGACCAAATCC
	MMP2	ATAACCTGGATGCCGTCGT	AGGCACCCTTGAAGAAGTAGC
	MMP9	GAACCAATCTCACCGACAGG	GCCACCCGAGTGTAACCATA
	PAI-1	TCCAGCAGCTGAATTCCTG	GCTGGAGACATCTGCATCCT
	Vimentin	AGATGGCCCTTGACATTGAG	TGGGTATCAACCAGAGGGAG
Mouse	α-SMA	ACTCTCTTCCAGCCATCTTTCA	ATAGGTGGTTTCGTGGATGC
	β-actin	CAGCTGAGAGGGAAATCGTG	CGTTGCCAATAGTGATGACC
	COL1A	CATGTTCAGCTTTGTGGACCT	GCAGCTGACTTCAGGGATGT
	FN	CGGAGAGAGTGCCCCTACTA	CGATATTGGTGAATCGCAGA
	FSP-1	GGAGCTGCCTAGCTTCCTG	TCCTGGAAGTCAACTTCATTGTC
	MMP2	TAACCTGGATGCCGTCGT	TTCAGGTAATAAGCACCCTTGAA
	MMP9	ACGACATAGACGGCATCCA	GCTGTGGTTCAGTTGTGGTG
	Vimentin	CCAACCTTTTCTTCCCTGAA	TGAGTGGGTGTCAACCAGAG

Samples were separated by SDS–PAGE, and then transferred to Hybond ECL nitrocellulose membrane (Amersham, USA). The membranes were incubated with primary antibodies α-tubulin (1:10 000), PAI-1 (1:1000), collagen IV (1:5000), fibronectin (1:1000), phospho-Smad2 (1:1000), phospho-Smad3 (1:1000), Smad3 (1:1000), ERK (1:1000), phospho-ERK (1:1000), phospho-p38 (1:1000), p38 (1:1000), phospho-JNK (1:1000) or JNK (1:1000) at 4°C overnight followed by HRP-conjugated secondary antibody (Amersham, UK) (1:5000). The blots were then detected with standard ECL technique, and the bands were quantified by densitometry using LAS-4000 Imaging System (FUJIFILM, Japan). Coomassie blue staining was used as loading control for cell culture supernatant samples and tubulin was used for cell lysates.

Gelatin zymography

Gelatin zymography was used to evaluate the effects of TRAM34 on the activity of gelatinases (MMP2 and MMP9). Briefly, cell supernatants containing an equal amount of total proteins were loaded into 10% SDS-polyacrylamide gel containing 1.0 mg/mL gelatin (Sigma). After electrophoresis, the gel was incubated at 25°C for 30 h in a developing buffer (50 mM Tris–HCl (pH 7.5), 10 mM $CaCl_2$, 100 mM NaCl and 0.02% NaN_3) prior to Coomassie blue staining. Destaining was performed in the same buffer devoid of Coomassie blue for 15 min. The unstained bands representing gelatinolytic activity were quantitated using densitometric analysis as described above.

Histology and immunohistochemistry

Paraffin-embedded sections were used for immunohistochemical staining. Matrix deposition within the interstitium was assessed using picrosirius red stain (Polysciences, PA, USA). For immnunohistochemistry staining, endogenous peroxidase activity was blocked by incubation in 0.3% hydrogen peroxide. After pre-incubation with 10% protein block (Dako, CA, USA) for 10 min at room temperature to block non-specific binding of antibodies, the tissues were incubated overnight at 4°C with primary antibodies against type I collagen, fibronectin and α-SMA. After incubation with appropriate secondary antibodies, sections were developed with 3,3-diaminobenzidine (Dako) to produce a brown color and counterstained with hematoxylin. Positive signals in the renal cortex regions were quantified using Image J software as previously described [23].

Statistical analysis

Results from at least three independent experiments were expressed as mean ± SEM. Statistical analysis of data from two groups was compared by two-tail *t*-test. Data from multiple groups were performed by one-way ANOVA, followed by Tukey post test. Statistical significance was determined as $P < 0.05$.

RESULTS

KCa3.1 blocker TRAM34 inhibits ECM gene expression and the activation of renal fibroblasts induced by TGF-β1 in human renal interstitial fibroblasts

To evaluate the role of KCa3.1 in fibroblastic activation, we used a highly selective inhibitor of KCa3.1, TRAM34, in human interstitial fibroblasts to investigate the effects of KCa3.1 inhibition on the expression of ECM genes following TGF-β1 exposure. Our pilot study has shown that for human interstitial fibroblasts, TRAM34 with 2 μM did not cause cytotoxicity by MTS assay but sufficiently inhibited KCa3.1 expression by qRT–PCR (data not shown). As shown in Figure 1A–C, TRAM34 significantly inhibited TGF-β1-induced mRNA expression of type I collagen ($P < 0.01$), type IV collagen ($P < 0.01$) and fibronectin ($P < 0.01$) in human renal interstitial fibroblasts. Western blot results further demonstrated that incubation with TRAM34 decreased the protein expression of type IV collagen ($P < 0.05$, Figure 1D) and fibronectin ($P <$

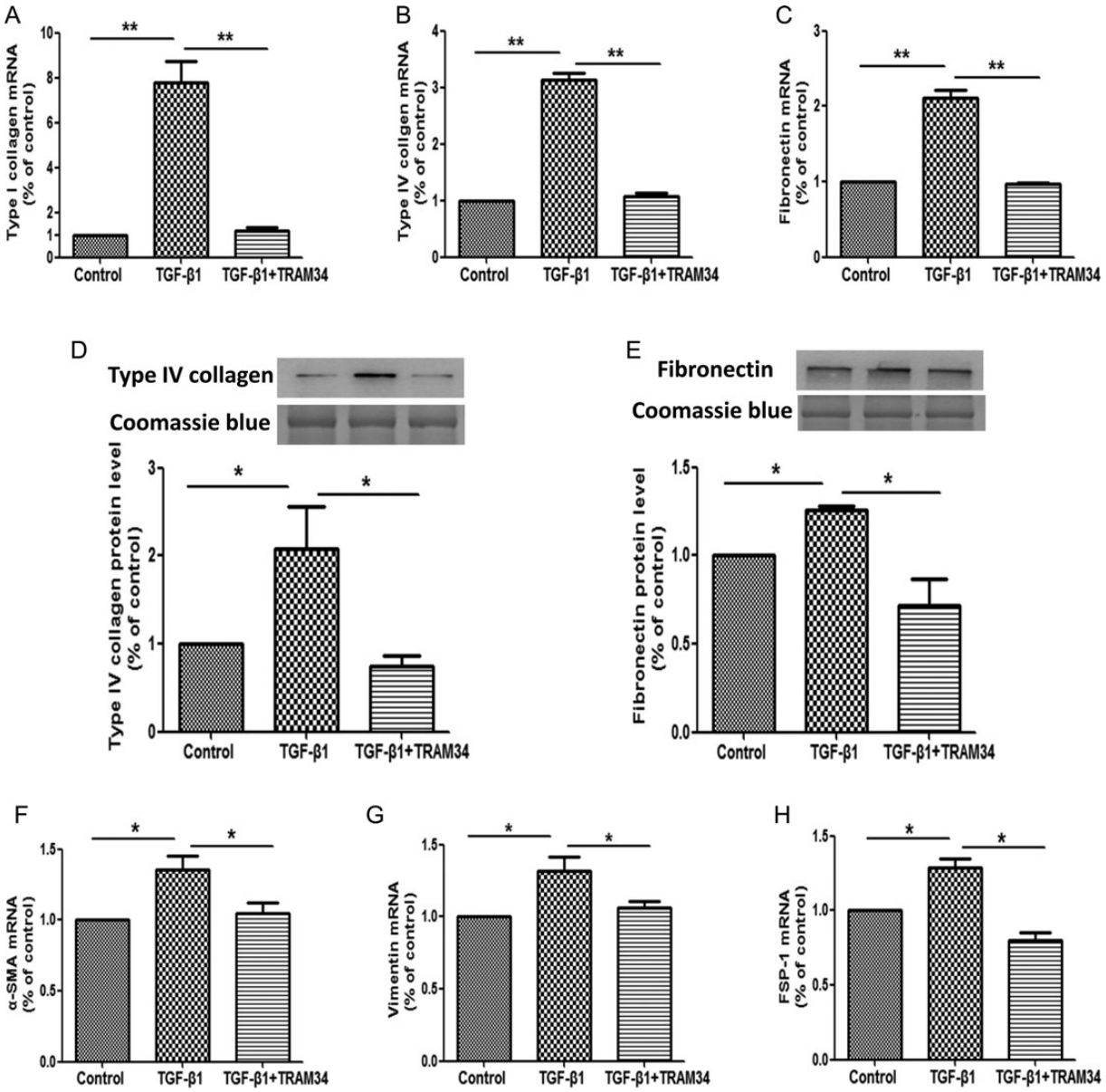

FIGURE 1: KCa3.1 blocker TRAM34 inhibited ECM gene expression and the activation of renal fibroblasts induced by TGF-β1 in human renal interstitial fibroblasts. Human renal interstitial fibroblasts were treated with control, TGF-β1 (2 ng/mL) or TGF-β1 (2 ng/mL) combined with TRAM34 (2 μM) for 48 h. Real-time RT–PCR results showed that TRAM34 inhibited TGF-β1-induced type I collagen (**A**), type IV collagen (**B**) and fibronectin (**C**) mRNA expression. Western blot results showed that TRAM34 inhibited the induction of type IV collagen (**D**) and fibronectin (**E**) in TGF-β1 treated human renal interstitial fibroblasts. Quantitative RT–PCR demonstrated TRAM34 reversed TGF-β1-induced α-SMA (**F**), vimentin (**G**) and FSP-1 mRNA (**H**). Results are presented as means ± SEM. *P < 0.05 and **P < 0.01, $n = 3$.

0.05, Figure 1E) in human interstitial fibroblasts exposed to TGF-β1.

Differentiation of fibroblasts into myofibroblasts represents a key process in tissue fibrogenesis [24]. Hence we sought to determine the effects of TRAM34 on myofibroblast activation in human interstitial fibroblasts. Markers of myofibroblast including α-SMA, vimentin and fibroblast-specific protein-1 (FSP-1) [25–27] were examined. TGF-β1 increased mRNA expression of α-SMA (P < 0.05, Figure 1F), vimentin (P < 0.05, Figure 1G) and FSP-1(P < 0.05, Figure 1H). Incubation with TRAM34 decreased TGF-β1-induced expression of α-SMA (P < 0.05), vimentin (P < 0.05) and FSP-1 (P < 0.05). Collectively, these data confirm the activation of renal fibroblasts induced by TGF-β1 and suggest that such activation can be reversed by concomitant inhibition of the KCa3.1 channel.

KCa3.1 blocker TRAM34 prevents TGF-β1-induced PAI-1 expression and activity of MMP2 and MMP9 in human renal interstitial fibroblasts

We then investigated in interstitial fibroblasts the effects of KCa3.1 inhibition on the expression of genes (PAI-1, MMP2 and MMP9), which are known to regulate ECM turnover following TGF-β1 exposure. Increased PAI-1 expression is widely recognized as being associated with the progression of chronic kidney diseases [28]. MMP2 and MMP9 are extracellular proteases responsible for the degradation of the ECM and other

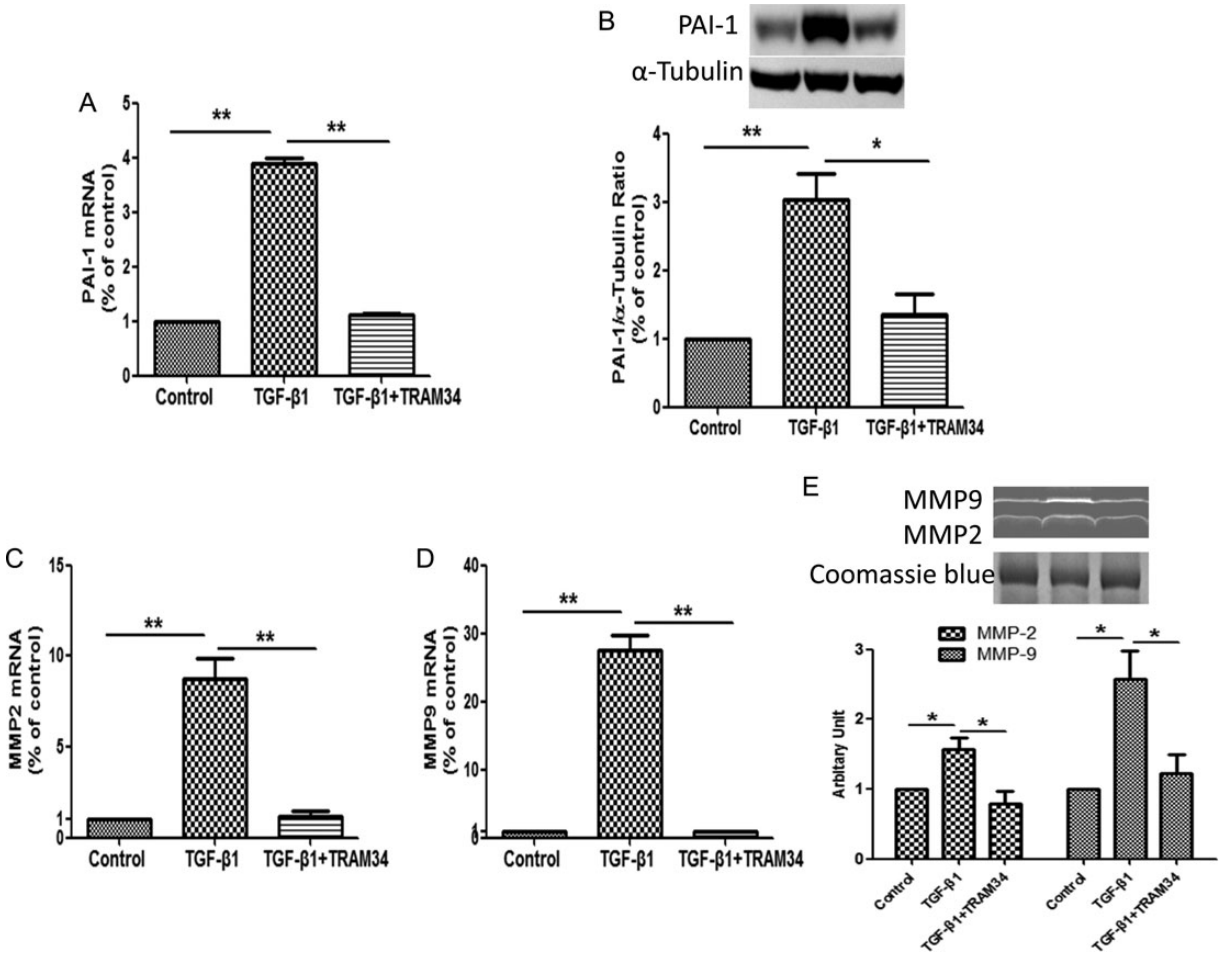

FIGURE 2: KCa3.1 blocker TRAM34 prevented TGF-β1-induced PAI-1, MMP2 and MMP9 expression in human renal interstitial fibroblasts. Human renal interstitial fibroblasts were treated with control, TGF-β1 (2 ng/mL) or TGF-β1 (2 ng/mL) combined with TRAM34 (2 μM) for 48 h. Quantitative RT–PCR and western blot results demonstrated TRAM34 suppressed TGF-β1-induced PAI-1 mRNA (**A**) and protein expression (**B**) as well as MMP2 (**C**) and MMP9 (**D**) mRNA expression in cultured human renal interstitial fibroblasts. (**E**) Zymographic analysis showed TRAM34 reversed TGF-β1-induced proteolytic activity of MMP2 and MMP9 in human renal interstitial fibroblasts. Results are presented as means ± SEM. *P < 0.05 and **P < 0.01, *n* = 3.

substrates during tissue remodeling. As shown in Figure 2A and B, TGF-β1 induced PAI-1 mRNA expression by 3.9-fold (P < 0.01) and protein by 3-fold (P < 0.01) in human renal interstitial fibroblasts, which were significantly inhibited by TRAM34 (P < 0.05). TGF-β1 also increased MMP2 and MMP9 mRNA levels by 8.8-fold and by 27.5-fold, respectively (P < 0.01, Figure 2C and D), with parallel increases in proteolytic activity analyzed by zymography (P < 0.05, Figure 2E). Co-incubation of renal interstitial fibroblasts with TRAM34 inhibited the induction of MMP2 and MMP9 by TGF-β1 (P < 0.05, Figure 2E). These data clearly indicate that KCa3.1 is also involved in mediating key fibrosis-related genes such as PAI-1, MMP2 and MMP9, known to be induced by TGF-β1.

KCa3.1 mediates TGF-β1 signaling via Smad or ERK1/2 pathways but not P38, JNK pathway in human renal interstitial fibroblasts

In order to further understand the mechanism whereby KCa3.1 influences TGF-β1 signaling in human renal interstitial fibroblasts, the effects of KCa3.1 on TGF-β1 signaling transduction pathways were investigated. As shown in Figure 3A and B, exposure of interstitial fibroblasts to TGF-β1 resulted in significantly increased Smad2 and Smad3 phosphorylation. TGF-β1-exposed cells exhibited over a 12-fold increase in p-Smad2 expression (P < 0.01) and over 2-fold increase in p-Smad3 expression (P < 0.01), respectively, when compared with control. Concurrent exposure to TRAM34 inhibited the TGF-β1-mediated increases in Smad2 (P < 0.01) and Smad3 expression (P < 0.01). TGF-β1 also increased the p-ERK1/2 expression by ~2-fold (P < 0.01), which was partially inhibited by TRAM34 in renal interstitial fibroblasts (P < 0.05) (Figure 3C). However, TRAM34 had no effect on the P38 and JNK MAP kinase pathways (Figure 3D and E).

Blockade of KCa3.1 improves renal injury in two STZ-induced diabetic models

We next sought to determine the role of KCa3.1 in DN using the two *in vivo* models of DN as described above. Urinary albumin excretion was 21.01 ± 3.59 mg/24 h in the KCa3.1+/+ control group and increased to 113.5 ± 11.68 mg/

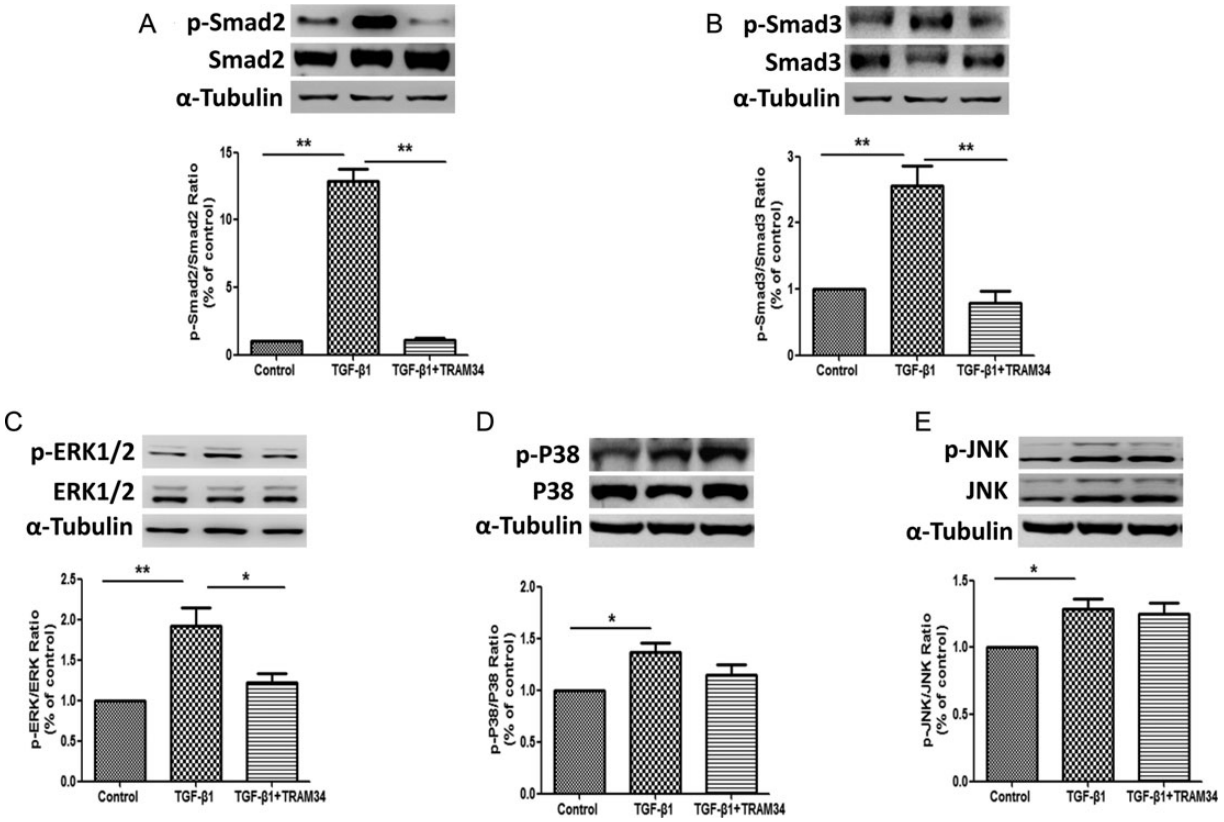

FIGURE 3: KCa3.1 mediated TGF-β1-induced activation of renal cortical fibroblasts and fibrotic responses through Smad and ERK pathway but not P38 and JNK pathways. Human renal interstitial fibroblasts were treated with control, TGF-β1 (2 ng/mL) or TGF-β1 (2 ng/mL) combined with TRAM34 (2 μM) for 48 h. Western blot results showed that TRAM34 inhibited the TGF-β1-mediated increases in p-Smad2 (**A**), p-Smad3 (**B**) expression and p-ERK1/2 expression (**C**). However, TRAM34 had no effect on the P38 (**D**) and JNK (**E**) MAP kinase pathways. Results are presented as means ± SEM. *P < 0.05 and **P < 0.01, *n* = 3.

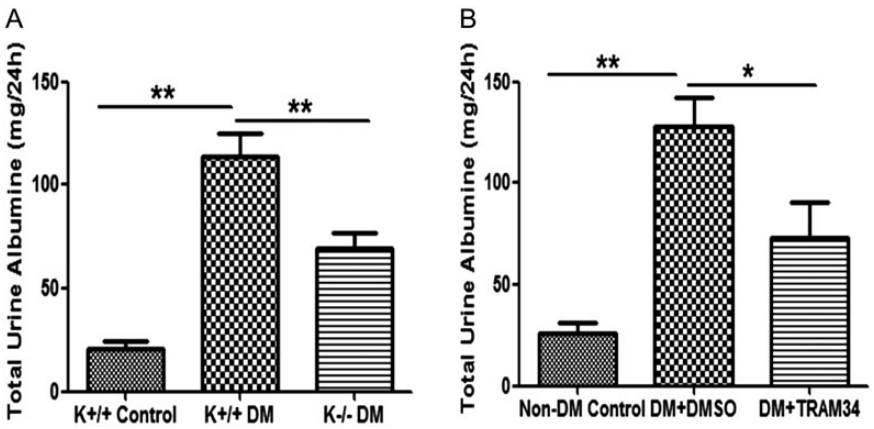

FIGURE 4: Blockade of KCa3.1 improved renal injury in two STZ-induced diabetic models. Two STZ-induced diabetic mouse models are used in this study: wild-type KCa3.1+/+ and KCa3.1−/− mice, and secondly eNOS−/− mice treated with or without a selective inhibitor of KCa3.1 (TRAM34). Kidney function was assessed by measuring the 24-h urinary albumin excretion. The 24-h urinary albumin excretion is significantly reduced in both KCa3.1-deficient mice (**A**) and eNOS−/− mice treated with TRAM34 (**B**). Results are presented as means ± SEM. *P < 0.05 and **P < 0.01, *n* = 6–8.

24 h (P < 0.01) in the KCa3.1+/+ diabetic group (Figure 4A). This effect was significantly reduced in KCa3.1−/− mice, to 69.48 ± 7.69 mg/24 h (P < 0.01, versus KCa3.1+/+ diabetic mice). Similar results were found with pharmacological inhibition of KCa3.1 in eNOS−/− diabetic mice following administration of TRAM34. Twenty-four-hour urinary albumin excretion was significantly increased in the diabetic mice (128.2 + 14.15 mg/24 h) compared with the non-diabetic

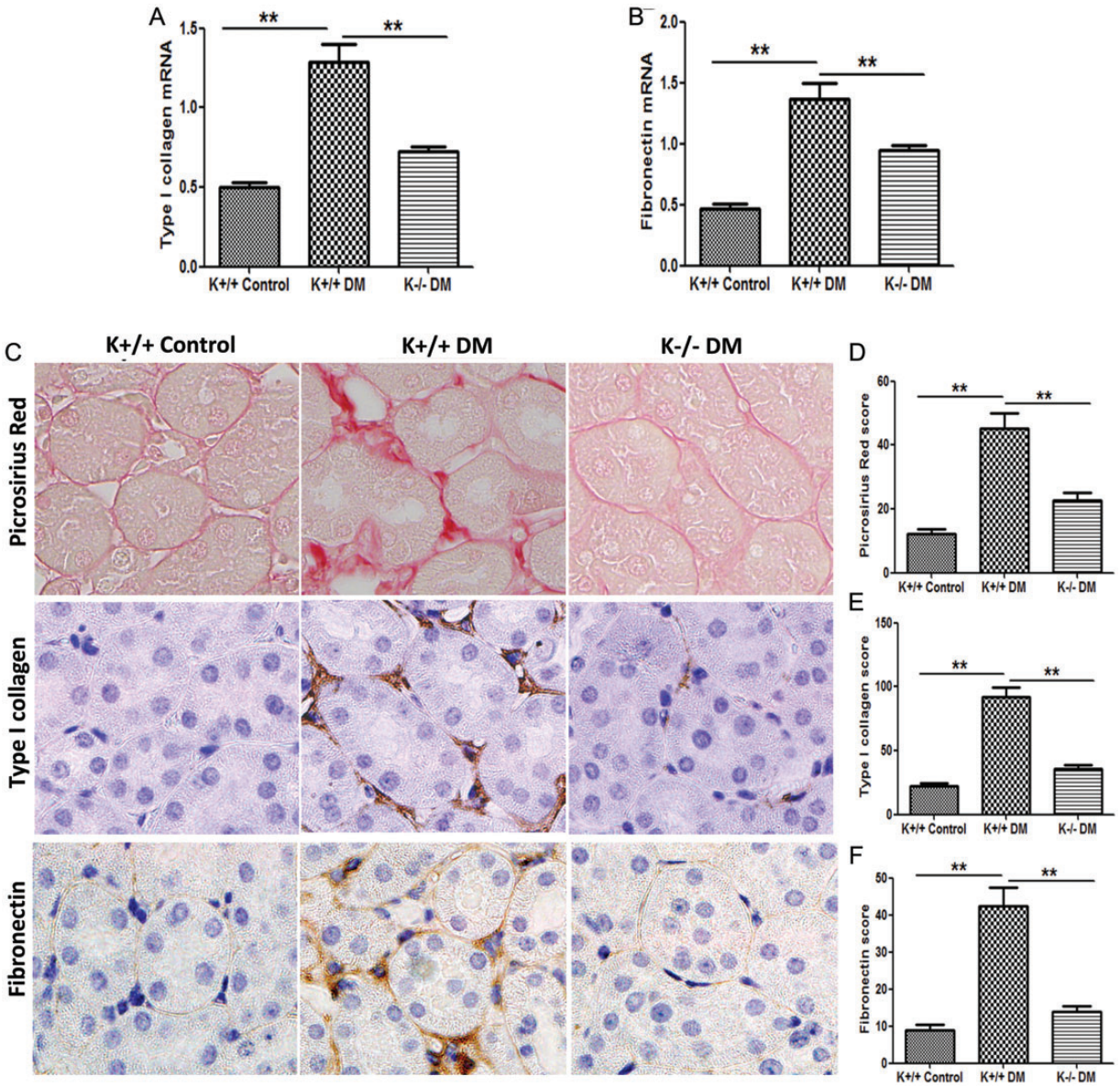

FIGURE 5: Blockade of KCa3.1 suppressed the overexpression of ECM in diabetic kidneys. Quantitative RT–PCR showed increased mRNA expression of type I collagen (**A**), and fibronectin (**B**) in the kidneys of KCa3.1+/+ diabetic mice compared with control mice but reduced in diabetic KCa3.1−/− kidneys ($n = 8$). Representative images (**C**) show picrosirius red and immunohistochemical staining of type I collagen and fibronectin in the renal cortex from control KCa3.1+/+ mice, KCa3.1+/+ diabetic mice and Kca3.1−/− diabetic mice ($n = 8$). Quantitative RT–PCR showed increased mRNA expression of type I collagen (**G**) and fibronectin (**H**) in the kidneys of diabetic eNOS−/− mice compared with control mice but reduced with TRAM34 treatment (DM+TRAM34) ($n = 6$). Representative images (**I**) show picrosirius red and immunohistochemical staining of type I collagen and fibronectin in the renal cortex from control mice, diabetic mice and diabetic mice treated with TRAM34. The degree of tubulointerstitial injury (**D** and **J**) and the quantitation of type I collagen (**E** and **K**) and fibronectin (**F** and **L**) were determined by computer-based morphometric analysis. Results are presented as mean ± SEM. *P < 0.05 and **P < 0.01. Original magnification: ×400.

control (25.72 ± 5.29 mg/24 h, P < 0.01), and this increase was significantly reduced by TRAM34 treatment (73.46 ± 16.69 mg/24 h, P < 0.05, Figure 4B).

Blockade of KCa3.1 represses matrix gene expression and reduces interstitial fibrosis in kidneys of diabetic mice

An increase in ECM protein is the major feature of renal fibrosis in DN [29, 30]. As shown in Figure 5A and B, a significant induction of type I collagen (2.8-fold, P < 0.01) and fibronectin (2.9-fold, P < 0.01) mRNA was observed in the kidneys of diabetic KCa3.1+/+ animals, when compared with non-diabetic controls. KCa3.1 deficiency significantly inhibited the expression of type I collagen and fibronectin in diabetic kidneys. Animals with diabetes mellitus demonstrated a marked increase in collagen deposition in the interstitial area of kidneys, as shown by picrosirius red staining (P < 0.01, Figure 5C and D). KCa3.1 deficiency significantly reduced excess matrix deposition (P < 0.01). In addition, diabetes mellitus resulted in increased expression of type I collagen (P

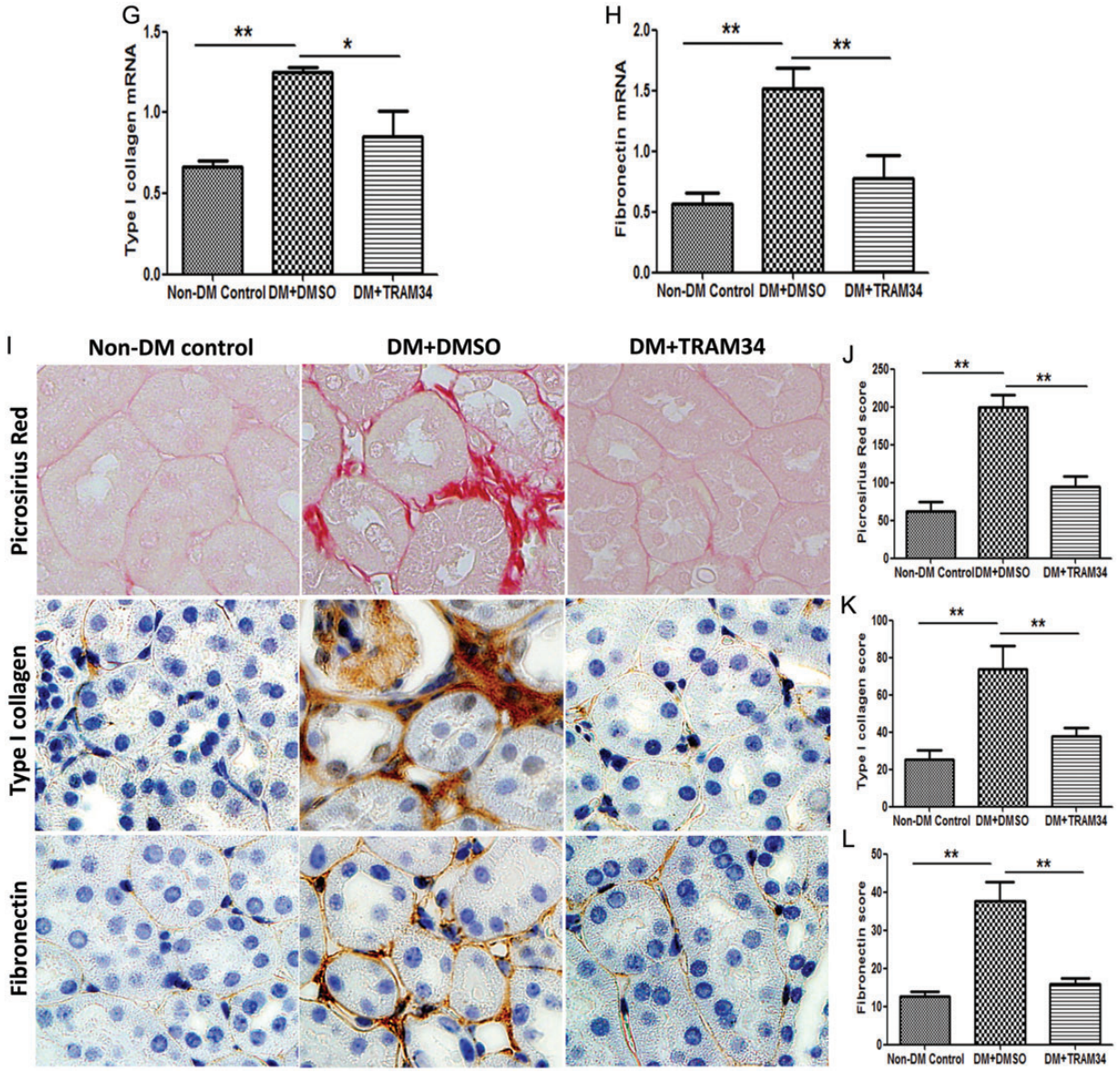

FIGURE 5: continued.

< 0.01, Figure 5C and E), and fibronectin ($P < 0.01$, Figure 5C and F) localized to the interstitial areas of diabetic kidneys, whereas KCa3.1 deficiency attenuated this response. Consistent with these observations, renal gene expression of type I collagen and fibronectin were considerably lower in diabetic kidneys from TRAM34-treated mice compared with vehicle-treated mice ($P < 0.01$, Figure 5G and H). Similarly, the administration of TRAM34 significantly reversed tubulointerstitial damage in diabetic kidneys when compared with vehicle-treated controls ($P < 0.01$, Figure 5I and J). Furthermore, immunohistochemical staining also showed substantially increased abundance of immunostainable type I collagen ($P < 0.01$, Figure 5I and K) and fibronectin ($P < 0.01$, Figure 5I and L) compared with controls, which was reversed after TRAM34 treatment. It is clear that blockade of KCa3.1 suppresses interstitial matrix overproduction and reduces renal fibrosis in *in vivo* models of DN.

Blockade of KCa3.1 reverses the activation of renal fibroblasts in kidneys of diabetic mice

We examined the effects of KCa3.1 on the activation of renal fibroblasts after exposure to conditions inherent in diabetes mellitus. RT–PCR analyses of kidney tissues demonstrated that the expression of α-SMA, vimentin and FSP-1 were increased by 1.9-fold, 1.8-fold and 2.2-fold, respectively, in diabetic KCa3.1+/+ mice, which were reduced in KCa3.1−/− diabetic mice ($P < 0.01$, Figure 6A–C). Consistently, histopathological analyses demonstrated an increased expression of α-SMA in kidneys of diabetic KCa3.1+/+ mice as compared with non-diabetic controls, which was significantly reversed in KCa3.1 deficient mice ($P < 0.01$, Figure 6D and E). We furthermore examined the effects of TRAM34 on fibroblast activation in the kidneys of diabetic mice. As shown in Figure 6F–H, the mRNA levels of α-SMA ($P < 0.01$), vimentin ($P < 0.01$) and FSP-1 ($P <$

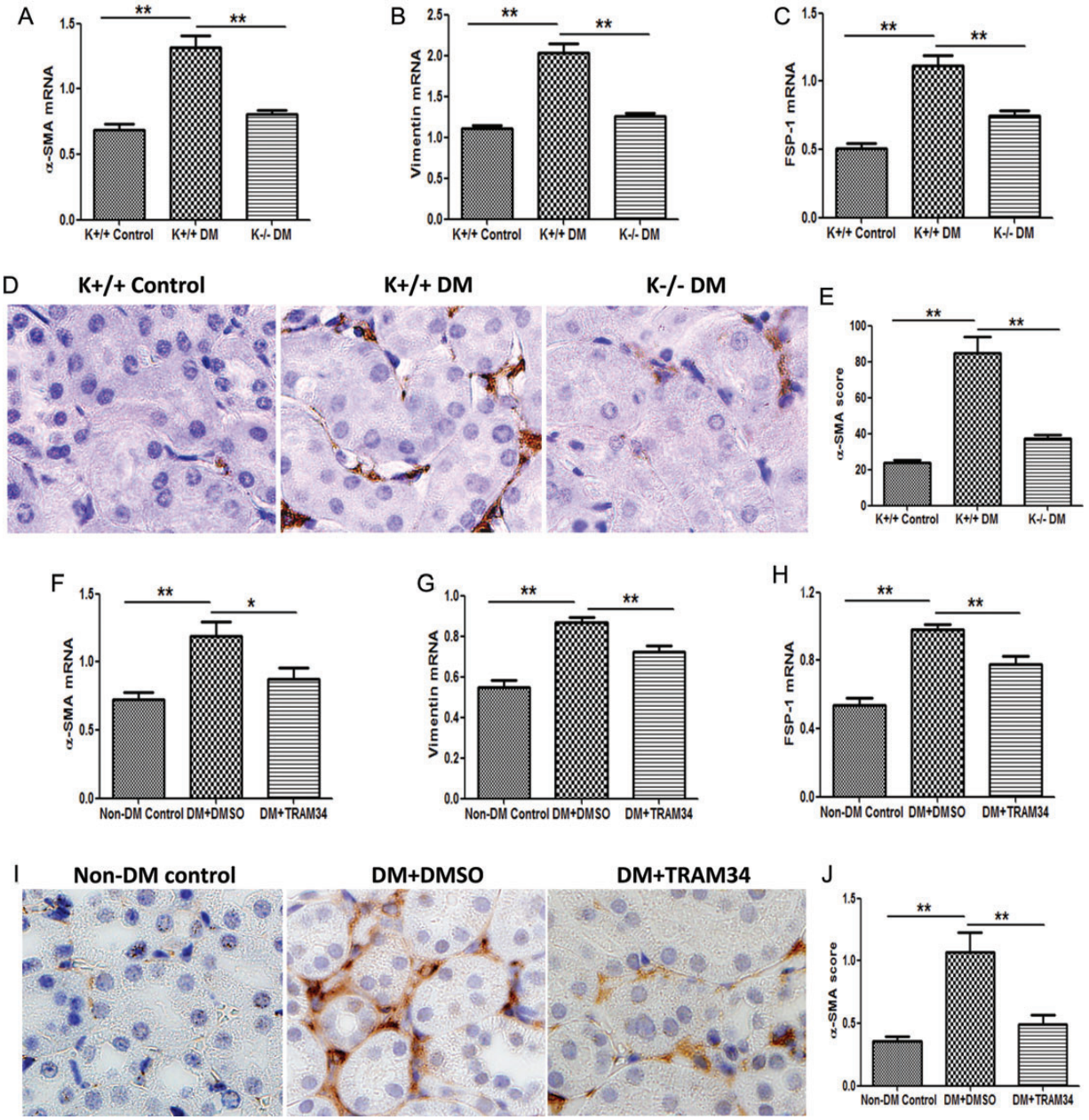

FIGURE 6: Blockade of KCa3.1 inhibited myofibroblast activation in kidneys of diabetic mice. Quantitative RT–PCR showed increased mRNA expression of α-SMA (**A**), vimentin (**B**) and FSP-1 (**C**) in the kidneys of diabetic KCa3.1+/+ mice compared with control mice but reduced in diabetic KCa3.1−/− kidneys ($n = 8$). (**D**) Immunohistochemical staining of α-SMA in the renal cortex from control KCa3.1+/+ mice, KCa3.1 +/+ diabetic mice and Kca3.1−/− diabetic mice ($n = 8$). Quantitative RT–PCR showed increased mRNA expression of α-SMA (**F**), vimentin (**G**) and FSP-1 (**H**) in the kidneys of eNOS−/− diabetic mice compared with control mice but reduced in diabetic kidneys treated with TRAM34 ($n = 6$). (**I**) Immunohistochemical staining of α-SMA in the renal cortex from control mice, diabetic mice and diabetic mice treated with TRAM34 ($n = 6$). The quantitation of α-SMA expression in mice kidneys (**E** and **J**). Results are presented as mean ± SEM. *P < 0.05 and **P < 0.01. Original magnification: ×400.

0.01) were significantly increased in the kidneys of diabetic mice compared with non-diabetic controls, which was mitigated by the administration of TRAM34. Immunohistochemical staining (Figure 6I) confirmed significantly increased α-SMA expression in diabetic kidneys compared with non-diabetic controls and TRAM34 suppressed α-SMA expression in kidneys of diabetic mice (P < 0.01, Figure 6J). Collectively, these data suggest that KCa3.1 is mechanistically involved in the activation of fibroblasts in DN *in vivo*.

Blockade of KCa3.1 represses MMP2 and MMP9 expression in kidneys of diabetic mice

We then investigated the consequences of KCa3.1 inhibition on the expression of fibrosis-related genes known to be relevant in kidney fibrosis. As indicated in Figure 7A and B, the mRNA expression of MMP2 and MMP9 was increased by 1.9-fold and 1.8-fold, respectively, in diabetic KCa3.1+/+ mice, which was reduced in KCa3.1−/− diabetic mice (P < 0.01). Consistent with this finding, we also observed a significant

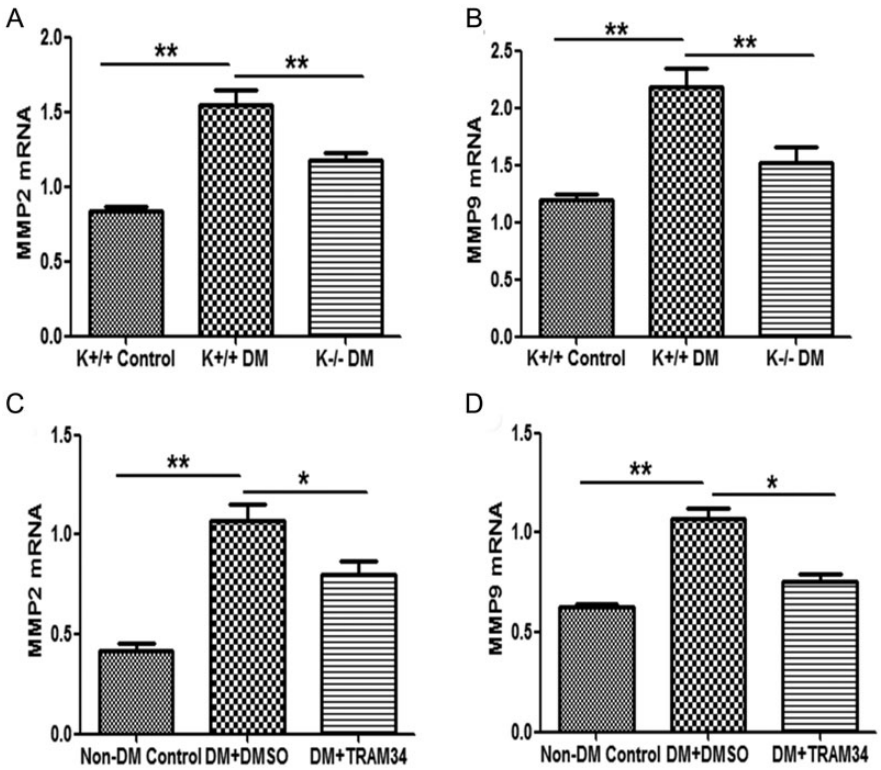

FIGURE 7: Blockade of KCa3.1 inhibited MMP2 and MMP9 expression in two STZ-induced diabetic models. Quantitative RT–PCR showed increased mRNA expression of MMP2 (**A**) and MMP9 (**B**) in the kidneys of diabetic KCa3.1+/+ mice compared with control mice but reduced in diabetic KCa3.1−/− kidneys ($n = 8$). Quantitative RT–PCR showed increased mRNA expression of MMP2 (**C**) and MMP9 (**D**) in the kidneys of eNOS−/− diabetic mice compared with control mice but reduced in diabetic kidneys treated with TRAM34 ($n = 6$). Results are presented as mean + SEM. *$P < 0.05$ and **$P < 0.01$.

decrease in the expression of MMP2 and MMP9 in the kidneys of diabetic eNOS−/− mice treated with the KCa3.1 blocker TRAM34 compared with vehicle-treated group ($P < 0.05$, Figure 7C and D). These data clearly indicate that KCa3.1 also plays a role in mediating several key genes elaborated by interstitial fibroblasts that regulate ECM accumulation *in vivo*.

DISCUSSION

This study was undertaken to define the role of KCa3.1 in the activation of renal fibroblasts in DN. This study shows that kidney fibroblast activation to myofibroblasts, characterized by acquisition of α-SMA phenotype and increased ECM, is regulated through KCa3.1. By using a small molecule inhibitor of the KCa3.1 pathway, we demonstrated that TRAM34, a highly selective inhibitor of KCa3.1, is able to protect human renal interstitial fibroblasts from TGF-β1 induction of activation of myofibroblasts and ECM production, which is likely to occur through Smad2/3 or ERK1/2 pathways, but independent of P38 or JNK pathways. Furthermore, blockade of KCa3.1 normalizes regulators of matrix production and matrix protein expression and thus reduces renal fibrosis in two animal models of DN. These effects were not only observed in KCa3.1 genetic deletion mice but also mice treated with the pharmacological KCa3.1 inhibitor TRAM34.

The activation of interstitial fibroblasts to become α-SMA-positive myofibroblasts is recognized as a key step in the evolution to chronic kidney disease. In addition to activated resident interstitial fibroblasts, myofibroblasts may also derive from tubular epithelial cells via an epithelial–mesenchymal transition (EMT) [31] or endothelial–mesenchymal transition [32], bone marrow-derived fibrocytes [33] and perivascular fibroblasts [34]. A recent report confirmed that total pool of myofibroblasts in fibrotic kidney consists of 50% local resident fibroblasts through proliferation, 35% non-proliferating myofibroblasts deriving through differentiation from bone marrow, 10% endothelial-to-mesenchymal transition program and 5% epithelial-to-mesenchymal transition program [35]. Regardless of the origin of myofibroblasts, these cells are considered to be primarily responsible for interstitial matrix accumulation and deposition [36]. Therefore, targeting the signaling pathways that mediates the activation of myofibroblasts may be a way to attenuate the progression of renal fibrosis in diabetes mellitus. In this study we found induction of diabetes increased the number of α-SMA-positive renal fibroblasts, while blockade of KCa3.1 significantly suppressed the activation of kidney fibroblasts, paralleled with a substantial reduction in ECM. These observations correlate with the findings of Grgic *et al.* [37], indicating the importance of KCa3.1 in mediating activation of renal interstitial fibroblasts and ultimately renal pathology. As has been reported in vascular smooth muscle cells [13], T lymphocytes [19] and cancer cells [38, 39],

KCa3.1 channel activation may promote fibroblast mitogenesis by enhancing the electrochemical driving force for Ca^{2+} influx through membrane hyperpolarization, thus sustaining the high intracellular Ca^{2+} concentration required for fibroblasts activation through gene transcription and DNA synthesis.

The association of TGF-β1 signaling pathways with myofibroblast activation in the pathogenesis of renal interstitial fibrosis is well documented. In fibroblasts, TGF-β1 regulation of α-SMA transcription and myofibroblast activation is mediated via phosphorylation of Smad2/3 that subsequently complexes with Smad4 and translocates to the nucleus, where the dimer binds to the promoter region of the α-SMA gene [40]. Studies also showed that ERK 1/2 MAPK signaling pathways act as an alternative pathway in TGF-β1 signaling. Interstitial fibroblasts express ERK1/2 in kidney fibrosis after unilateral ureteral obstruction that can be ameliorated by inhibitors of ERK1/2 [41]. In other cell types like human lung fibroblasts, the activation of p38 and JNK signaling pathways were found to be involved in fibroblast activation stimulated by TGF-β1. Therefore, the regulation of Smad, ERK1/2, p38 and JNK MAPK in fibroblast activation is cell and tissue specific. In this study, we found that blockade of KCa3.1 inhibited the activation of Smad2, Smad3 and Erk1/2 signaling pathways, but not p38 and JNK MAPK pathways, indicating that KCa3.1 plays an important role involving Smad2, Smad3 and ERK1/2 in kidney myofibroblast activation by TGF-β1.

Increased ECM protein synthesis and/or decreased ECM degradation ultimately contributes to the development of diabetes-associated tubulointerstitial fibrosis [4, 42]. Thus, attenuating ECM accumulation and/or enhancing ECM degradation is considered a prime target in the treatment of diabetic renal complications. It is well known that MMP2 and MMP9 play an important role in ECM deposition in tubulointerstitial fibrosis [29]. It was demonstrated that the increased activity of MMP2 and MMP9 degrade tubular basement membranes and promote fibrosis by facilitating tubular cell EMT, which is regarded as a direct contributor to the kidney myofibroblast population in the development of renal fibrosis, specifically in DN [43–45]. In the present study, we showed that diabetes is associated with an increase in MMP2 and MMP9 expression and blockade of KCa3.1 attenuates diabetes-induced MMP2 and MMP9 expression, indicating that this may be one of the mechanism by which the antifibrotic effect of KCa3.1 inhibition is exerted in the diabetic kidney.

In summary, the present study further demonstrates that, in the STZ-induced diabetic mice, blockade of KCa3.1 is renoprotective by attenuating albuminuria and ECM protein expression associated with diabetic tubulointerstitial fibrosis. The mechanisms by which KCa3.1 inhibition exerts its antifibrotic effects in diabetes are suppression of activation of renal interstitial fibroblasts and regulation of the expression of fibrotic related genes expressed by fibroblasts such as MMP2 and MMP9. Given that KCa3.1 blockade limits ECM production in both proximal tubular cells and fibroblasts, the opportunity for therapeutic potential should be explored.

ACKNOWLEDGEMENTS

The KCa3.1−/− mice were kindly provided by Dr James Melvin, National Institute of Dental and Craniofacial Research, Bethesda, MD, USA. This work was supported by Australian National Health and Medical Research Council Project grant (NHMRC APP1025918) and University of Sydney Postgraduate Award (C.H.).

CONFLICT OF INTEREST STATEMENT

None declared.

REFERENCES

1. Zeisberg M, Neilson EG. Mechanisms of tubulointerstitial fibrosis. J Am Soc Nephrol 2010; 21: 1819–1834
2. Desmouliere A, Darby IA, Gabbiani G. Normal and pathologic soft tissue remodeling: role of the myofibroblast, with special emphasis on liver and kidney fibrosis. Lab Invest 2003; 83: 1689–1707
3. Lan HY. Diverse roles of TGF-beta/Smads in renal fibrosis and inflammation. Int J Biol Sci 2011; 7: 1056–1067
4. Wolf G. Growth factors and the development of diabetic nephropathy. Curr Diab Rep 2003; 3: 485–490
5. Prud'homme GJ. Pathobiology of transforming growth factor beta in cancer, fibrosis and immunologic disease, and therapeutic considerations. Lab Invest 2007; 87: 1077–1091
6. Krag S, Danielsen CC, Carmeliet P *et al.* Plasminogen activator inhibitor-1 gene deficiency attenuates TGF-beta1-induced kidney disease. Kidney Int 2005; 68: 2651–2666
7. Hwang M, Kim HJ, Noh HJ *et al.* TGF-beta1 siRNA suppresses the tubulointerstitial fibrosis in the kidney of ureteral obstruction. Exp Mol Pathol 2006; 81: 48–54
8. Chou CC, Lunn CA, Murgolo NJ. KCa3.1: target and marker for cancer, autoimmune disorder and vascular inflammation? Expert Rev Mol Diagn 2008; 8: 179–187
9. Hu L, Pennington M, Jiang Q *et al.* Characterization of the functional properties of the voltage-gated potassium channel Kv1.3 in human CD4+ T lymphocytes. J Immunol 2007; 179: 4563–4570
10. Tao R, Lau CP, Tse HF *et al.* Regulation of cell proliferation by intermediate-conductance Ca^{2+}-activated potassium and volume-sensitive chloride channels in mouse mesenchymal stem cells. Am J Physiol Cell Physiol 2008; 295: C1409–C1416
11. Tharp DL, Bowles DK. The intermediate-conductance Ca^{2+} -activated K^+ channel (KCa3.1) in vascular disease. Cardiovasc Hematol Agents Med Chem 2009; 7: 1–11
12. Toyama K, Wulff H, Chandy KG *et al.* The intermediate-conductance calcium-activated potassium channel KCa3.1 contributes to atherogenesis in mice and humans. J Clin Invest 2008; 118: 3025–3037
13. Kohler R, Wulff H, Eichler I *et al.* Blockade of the intermediate-conductance calcium-activated potassium channel as a new therapeutic strategy for restenosis. Circulation 2003; 108: 1119–1125
14. Wulff H, Kolski-Andreaco A, Sankaranarayanan A *et al.* Modulators of small- and intermediate-conductance calcium-activated potassium channels and their therapeutic indications. Curr Med Chem 2007; 14: 1437–1457
15. Ohya S, Kimura K, Niwa S *et al.* Malignancy grade-dependent expression of K^+-channel subtypes in human prostate cancer. J Pharmacol Sci 2009; 109: 148–151
16. Huang C, Shen S, Ma Q *et al.* Blockade of KCa3.1 ameliorates renal fibrosis through a TGF-b1/Smad pathway in diabetic mice. Diabetes 2013; 62: 2923–2934
17. Johnson DW, Saunders HJ, Brew BK *et al.* Human renal fibroblasts modulate proximal tubule cell growth and transport via the IGF-I axis. Kidney Int 1997; 52: 1486–1496

18. Wulff H, Gutman GA, Cahalan MD *et al.* Delineation of the clotrimazole/TRAM-34 binding site on the intermediate conductance calcium-activated potassium channel, IKCa1. J Biol Chem 2001; 276: 32040–32045
19. Wulff H, Miller MJ, Hansel W *et al.* Design of a potent and selective inhibitor of the intermediate-conductance Ca^{2+}-activated K^+ channel, IKCa1: a potential immunosuppressant. Proc Natl Acad Sci USA 2000; 97: 8151–8156
20. Brosius FC, III, Alpers CE, Bottinger EP *et al.* Mouse models of diabetic nephropathy. J Am Soc Nephrol 2009; 20: 2503–2512
21. Tesch GH, Allen TJ. Rodent models of streptozotocin-induced diabetic nephropathy. Nephrology (Carlton) 2007; 12: 261–266
22. Livak KJ, Schmittgen TD. Analysis of relative gene expression data using real-time quantitative PCR and the 2(T)(-Delta Delta C) method. Methods 2001; 25: 402–408
23. Doi S, Zou Y, Togao O *et al.* Klotho inhibits transforming growth factor-beta1 (TGF-beta1) signaling and suppresses renal fibrosis and cancer metastasis in mice. J Biol Chem 2011; 286: 8655–8665
24. Ghosh AK, Vaughan DE. PAI-1 in tissue fibrosis. J Cell Physiol 2012; 227: 493–507
25. Hewitson TD. Renal tubulointerstitial fibrosis: common but never simple. Am J Physiol Renal Physiol 2009; 296: F1239–F1244
26. Iwano M, Plieth D, Danoff TM *et al.* Evidence that fibroblasts derive from epithelium during tissue fibrosis. J Clin Invest 2002; 110: 341–350
27. Huang Y, Noble NA. PAI-1 as a target in kidney disease. Curr Drug Targets 2007; 8: 1007–1015
28. Eddy AA, Fogo AB. Plasminogen activator inhibitor-1 in chronic kidney disease: evidence and mechanisms of action. J Am Soc Nephrol 2006; 17: 2999–3012
29. Catania JM, Chen G, Parrish AR. Role of matrix metalloproteinases in renal pathophysiologies. Am J Physiol Renal Physiol 2007; 292: F905–F911
30. Heeg MH, Koziolek MJ, Vasko R *et al.* The antifibrotic effects of relaxin in human renal fibroblasts are mediated in part by inhibition of the Smad2 pathway. Kidney Int 2005; 68: 96–109
31. Yamashita S, Maeshima A, Nojima Y. Involvement of renal progenitor tubular cells in epithelial-to-mesenchymal transition in fibrotic rat kidneys. J Am Soc Nephrol 2005; 16: 2044–2051
32. Li J, Qu X, Bertram JF. Endothelial-myofibroblast transition contributes to the early development of diabetic renal interstitial fibrosis in streptozotocin-induced diabetic mice. Am J Pathol 2009; 175: 1380–1388
33. Li J, Deane JA, Campanale NV *et al.* The contribution of bone marrow-derived cells to the development of renal interstitial fibrosis. Stem Cells 2007; 25: 697–706
34. Lin SL, Kisseleva T, Brenner DA *et al.* Pericytes and perivascular fibroblasts are the primary source of collagen-producing cells in obstructive fibrosis of the kidney. Am J Pathol 2008; 173: 1617–1627
35. Lebleu VS, Taduri G, O'Connell J *et al.* Origin and function of myofibroblasts in kidney fibrosis. Nat Med 2013; 19: 1047–1053
36. Liu Y. Renal fibrosis: new insights into the pathogenesis and therapeutics. Kidney Int 2006; 69: 213–217
37. Grgic I, Kiss E, Kaistha BP *et al.* Renal fibrosis is attenuated by targeted disruption of KCa3.1 potassium channels. Proc Natl Acad Sci USA 2009; 106: 14518–14523
38. Ouadid-Ahidouch H, Roudbaraki M, Delcourt P *et al.* Functional and molecular identification of intermediate-conductance Ca(2+)-activated K(+) channels in breast cancer cells: association with cell cycle progression. Am J Physiol Cell Physiol 2004; 287: C125–C134
39. Jager H, Dreker T, Buck A *et al.* Blockage of intermediate-conductance Ca^{2+}-activated K^+ channels inhibit human pancreatic cancer cell growth in vitro. Mol Pharmacol 2004; 65: 630–638
40. Hinz B. Formation and function of the myofibroblast during tissue repair. J Invest Dermatol 2007; 127: 526–537
41. Rodriguez-Pena AB, Grande MT, Eleno N *et al.* Activation of Erk1/2 and Akt following unilateral ureteral obstruction. Kidney Int 2008; 74: 196–209
42. Mankhey RW, Bhatti F, Maric C. 17beta-Estradiol Replacement improves renal function and pathology associated with diabetic nephropathy. Am J Physiol Renal Physiol 2005; 288: F399–F405
43. Cheng S, Lovett DH. Gelatinase A (MMP-2) is necessary and sufficient for renal tubular cell epithelial-mesenchymal transformation. Am J Pathol 2003; 162: 1937–1949
44. Tan TK, Zheng G, Hsu TT *et al.* Macrophage matrix metalloproteinase-9 mediates epithelial-mesenchymal transition in vitro in murine renal tubular cells. Am J Pathol 2010; 176: 1256–1270
45. Kalluri R. EMT: when epithelial cells decide to become mesenchymal-like cells. J Clin Invest 2009; 119: 1417–1419

Received for publication: 19.6.2013; Accepted in revised form: 5.9.2013